Clay-Based Nanocomposite Coating for Flexible Optoelectronics Applying Commercial Polymers

Daniel A. Kunz,[†] Jasmin Schmid,[†] Patrick Feicht,[†] Johann Erath,[‡] Andreas Fery,[‡] and Josef Breu[†,*]

[†]Department of Inorganic Chemistry I, University of Bayreuth, Universitätsstraße 30, 95440 Bayreuth, Germany and [‡]Department of Physical Chemistry II, University of Bayreuth, Universitätsstraße 30, D-95440 Bayreuth, Germany

ABSTRACT Transparency, flexibility, and especially ultralow oxygen (OTR) and water vapor (WVTR) transmission rates are the key issues to be addressed for packaging of flexible organic photovoltaics and organic light-emitting diodes. Concomitant optimization of all essential features is still a big challenge. Here we present a thin (1.5 μm), highly transparent, and at the same time flexible nanocomposite coating with an exceptionally low OTR and WVTR (1.0×10^{-2} cm^3 m^{-2} day^{-1} bar^{-1} and <0.05 g m^{-2} day^{-1} at 50% RH, respectively). A commercially available polyurethane (Desmodur N 3600 and Desmophen 670 BA, Bayer MaterialScience AG) was filled with a delaminated synthetic layered silicate exhibiting huge aspect ratios of about 25 000. Functional films were prepared by simple doctor-blading a suspension of the matrix and the organophilized clay. This preparation procedure is technically benign, is easy to scale up, and may readily be applied for encapsulation of sensitive flexible electronics.

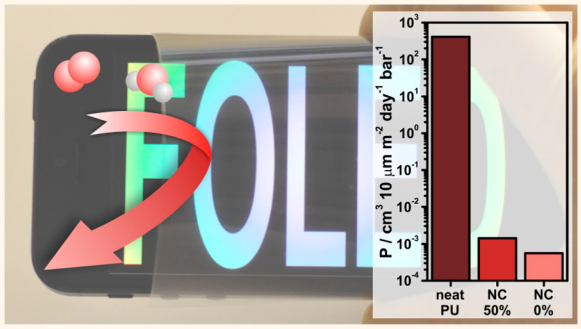

KEYWORDS: OLED · OPV · oxygen barrier · water vapor barrier · nanocomposite · coating · layered silicate

Efficient and thin coatings with a high barrier to various gases and fluids are needed for a wide range of applications stretching from food packaging[1,2] to high-tech applications such as flexible display packaging.[3−5] Flexible organic photovoltaics (FOPVs) and flexible organic light-emitting diodes (FOLEDs) are superior to conventional devices with respect to their multifunctionality, high durability, and impact resistance and are currently intensively studied. Molecular compounds applied in both FOPVs and FOLEDs suffer, however, from oxygen and moisture sensitivity. Efficient and sufficiently flexible barrier coatings are consequently a major challenge faced by the flexible electronics industry.[6] In order to achieve sufficient performance and lifetime, it has been estimated that transparent coatings need to limit the oxygen transmission rate (OTR) below 10^{-5} cm^3 m^{-2} day^{-1} bar^{-1} and a water vapor transmission rate (WVTR) below 10^{-6} g m^{-2} day^{-1} for application in reliable FOLEDs.[7] The requirements for FOPV are slightly less stringent (OTR < 10^{-3} cm^3 m^{-2} day^{-1} bar^{-1} and WVTR < 10^{-4} g m^{-2} day^{-1}, respectively). State of the art encapsulation with vapor-deposited thin films consisting of SiO_x or Al_2O_3 provide a sufficient barrier but are prone to cracks when flexed.

It has been shown that nanocomposites consisting of platy inorganic fillers such as clays embedded in a polymeric matrix provide sufficient flexibility and excellent mechanical properties mimicking nacre.[8,9] According to tortuous path theory, the performance of nanocomposite coatings as gas barriers is determined by the aspect ratio and the filler content. The maximum reduction that may theoretically be achieved by impermeable platelets due to the elongation of the diffusion path is described by various tortuous path models, *e.g.*, the Cussler model (Figure 1). Here the relative permeability (P_{rel}) is determined as

$$P_{rel} = \frac{P}{P_0} = \left(1+\mu \frac{\alpha^2\phi^2}{1-\phi}\right)^{-1} \quad (1)$$

where P/P_0 is the ratio of the permeability of the filled and unfilled polymer matrix,

* Address correspondence to josef.breu@uni-bayreuth.de.

Received for review February 14, 2013 and accepted April 1, 2013.

Published online April 02, 2013
10.1021/nn400713e

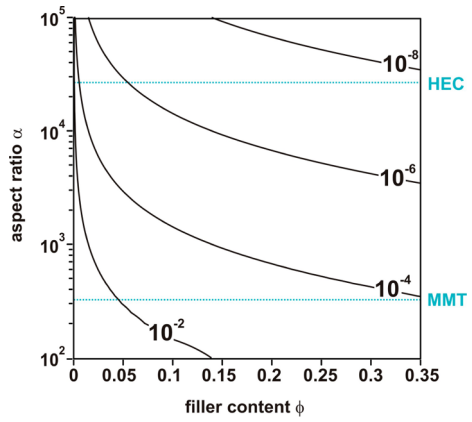

Figure 1. Relative permeability as function of aspect ratio and filler content according to Cussler's model. Dashed turquoise lines mark maximum aspect ratios of natural montmorillonite (MMT, <300) and the applied synthetic hectorite (HEC, ~25 000), respectively.

respectively. ϕ represents the filler content and α the aspect ratio of the filler. μ is a geometric factor with a value of 4/9 in the case of hexagonal platelets.[10]

The most efficient and elegant way to maximize the aspect ratio is to take advantage of the intracrystalline reactivity of layered compounds. At best, so-called osmotic swelling of interlayer cations in materials such as graphene oxide or clay minerals leads to spontaneous delamination into singular platelets of thickness smaller than 1 nm.[11−14] In this fortunate case, the aspect ratio is limited only by the lateral extension of the tactoids, which is determined by crystallization/synthesis conditions. While synthetic hectorites can be obtained in dimensions up to 20 μm[14] and are perfectly transparent, tactoids of natural clays such as montmorillonite are smaller than 300 nm and are colored due to iron impurities. In roll-to-roll processing, nanocomposite film thicknesses of typically <10 μm can be applied. A neat film of the commercial polyurethane applied here shows an OTR of 409.4 cm^3 m^{-2} day^{-1} bar^{-1} (normalized to 10 μm). For a functional film to meet the FOLED criteria cited above, the relative permeability must be reduced to 10^{-8}.

Organically modified montmorillonites such as Cloisite 93 show a *d*-spacing of 2.79 nm. A singular clay layer itself is 0.96 nm.[15,16] Thus for this intercalation compound, with a strictly alternating sequence of clay layer and organic alkylammonium counterions, the "filler content" is 35 vol %. This filler content may therefore be regarded as an upper limit for nanocomposites of delaminated clays that may be processed. Practically, for processability reasons this value will be even further reduced. Consequently, as depicted in Figure 1, composites containing natural clays such as montmorillonite (MMT) cannot meet the relative permeability requirements due to their limited lateral dimension. Even at maximum filler content and with perfectly delaminated MMT, only a maximum reduction of the permeability of the polymer matrix by 4 orders of magnitude can be achieved. Furthermore, natural clays often carry significant amounts of globular accessorial impurities, which may act as defects that will further enhance the permeability. Reduction of the relative permeability by 8 orders of magnitude would require an effective aspect ratio of 35 000 at a filler content of 35 vol %.

Tortuous path theory assumes that the OTR of the matrix volume in composites is not affected by the presence of the filler. This assumption is of course a rather crude approximation in such highly filled nanocomposites. Completely delaminated clay typically will show some 800 m^2 g^{-1} surface, which is transformed into interface when perfectly dispersed into the polymer matrix. Possible changes of free volume at the interface are therefore expected to crucially affect the OTR of the composite.[17] This is, however, completely neglected by tortuous path theory. Furthermore, the hydrophilic nature of the pristine clay minerals requires hydrophobization of the surfaces for two reasons: to reduce water vapor solubility in the composite and to avoid defects between filler and matrix due to marked differences in the surface tension. Along this line, dip-coating allows for composite formation and organophilization *via* "Umladung" (charge reversal) in consecutive dipping steps.[8,9,18−22] A bilayer thickness is, however, typically limited to about 5 nm,[21] and sufficiently thick functional films require many dipping steps.

In this work we report on a highly efficient, transparent, and flexible nanocomposite coating consisting of organophilized synthetic clay nanoplatelets embedded in a commercially available polyurethane matrix.

RESULTS AND DISCUSSION

On the basis of a recent breakthrough in the synthesis of a $Na_{0.5}$-fluorohectorite ($Na_{0.5}(Mg_{2.5}Li_{0.5})Si_4O_{10}F_2$, denoted as Na-hec) we were able to apply a filler material that is unique with respect to homogeneity, purity, and particle size.[14] Furthermore, Na-hec shows osmotic swelling when thrown into deionized water, causing spontaneous delamination, *i.e.*, disintegration into single clay lamellae. Due to this gentle and elegant anisotropic top-down process, unprecedented ultrahigh aspect ratios can be easily achieved.

The number-weighted lateral extension of the batch of clay platelets used as filler was determined by focused beam reflectance measurements (FBRM).[23] The measurements were first performed in aqueous dispersions; the particle size distribution therefore is representative for the bulk material. Moreover, it has been shown by Goossens[24] that the lateral extensions of clay tactoids correlate well with the hydrodynamical radius. We are, however, aware that the absolute values might be somewhat in error because of the large size

and the floppy nature of the nanoplatelets. Considering a platelet thickness of about 1 nm and a median lateral extension of the clay particles of 25 μm (Figure S1, Supporting Information) and assuming complete delamination by osmotic swelling, $Na_{0.5}$-Hec offers a mean aspect ratio of 25 000, which is about 80 times higher than the largest platelets of MMT.

As mentioned before, incorporation of these platelets into the polymer matrix, however, requires compatibilization of the filler. Insufficient adjustment of the interface is expected to increase the free volume and/or foster aggregation of platelets, resulting in a lower barrier activity. Organophilization was achieved by a simple cation exchange, replacing Na^+ against quaternized dimethylaminoethyl methacrylate (TMAEMA). This particular modifier allows for a subtle adjustment of surface tension. While cation exchange with standard modifiers such as quaterny ammonium cations causes immediate flocculation, this particular modifier allows maintaining a good dispersibility in water with no signs of aggregation. Rather flocculation of the organophilized fluorohectorite (O-hec) can be triggered in a controlled way by adding the hydrous dispersion into a 10/1 THF/butanone mixture. The precipitate is filtered and can then be completely redispersed in a polar organic solvent such as acetonitrile. The quality of the redispersion was cross-checked by FBRM particle size analysis. No larger aggregates were found (24 μm median value; see Figure S1, Supporting Information).

The O-hec suspension in acetonitrile (8.8 mg mL^{-1}) was subsequently mixed with a standard, commercially available two-component polyurethane precursor polymer system (Desmodur N 3600 and Desmophen 670 BA, Bayer MaterialScience AG). The amount of suspension added corresponded to a final filler content of 50 wt % (*ca.* 30 vol %) based on solvent-free nanocomposite and pristine, nonmodified filler. The nanocomposite suspension was doctor-bladed on a 100 μm thick polyethylene terephthalate (PET) foil and finally dried and hardened. Figure 2 summarizes the critical steps involved in the described procedure.

Doctor-blading as a coating technique is advantageous compared to conventional layer-by-layer techniques since it allows for preparation of larger area coatings in a fraction of the time because film thicknesses of 1−2 μm can be achieved in one step. Moreover, a highly lamellar orientation of the nanoplatelets is achieved by shear forces acting during the coating process and by the ultrahigh aspect ratio of the filler. A cross sectional scanning microscopy (SEM) image underlines the very good texture (Figure 3a).

Unfortunately, due to the relatively high filler content aimed at, the filler cannot be dispersed in the neat precursor polymer, and additional solvent is indispensable to maintain a viscosity of the nanocomposite suspension that allows processing. While in layer-by-layer fabrication, bilayers of 5 nm have to be dried between

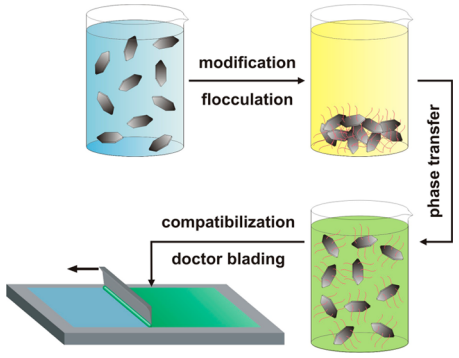

Figure 2. Experimental procedure for fabrication of large-scale nanocomposite coatings. An organophilization (modification and flocculation) step, followed by a phase transfer into a compatible solvent, is conducted. After mixing with commercially available polyurethane precursor polymers the coating is generated *via* scalable doctor-blading with subsequent drying and hardening.

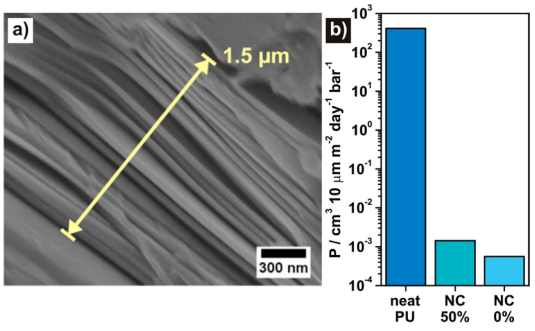

Figure 3. (a) SEM cross section of the nanocomposite coating. (b) Measured permeabilities of the neat polyurethane coating (neat PU) and of the nanocomposite coating (NC) at 50% and 0% RH, respectively. All values are decoupled from the supporting PET foil according to a literature procedure.[26]

steps, in doctor-blading 300 times more solvent has to be able to escape from the 1.5 μm thick film. Drying of the film is therefore a very critical step, even more so, as the barrier film is self-sealing as drying and hardening proceeds from the outer layers to the core. Too fast and uncontrolled drying can cause blisters in the coating, which act as defects and ruin the gas barrier properties.[25] The commercial two-component polyurethane system was deliberately chosen with these difficulties in mind. The gel-like behavior of the nonhardened precursor polymers freezes the orientation and location of the nanoplatelets but allows for outgassing of the volatile solvent within the given curing time (3 days at 80 °C) of the precursors. With that approach blister-free nanocomposite coatings with no detectable amounts of entrapped solvent were obtained.

OTR measurements of the nanocomposite coating were conducted at 25 °C and relative humidities of 0% and 50%, respectively. It is noteworthy that absolute OTR values of 3.7×10^{-3} cm^3 m^{-2} day^{-1} bar^{-1} are below the detection limit of commercially available equipment and had to be measured with a new

TABLE 1. OTR Values and Calculated Permeability (*P*) of the Nanocomposite Coating at Different RH in Comparison with Neat PET Foil and Neat Polyurethane Coating on PET[a]

				P/cm^3 10 μm m^{-2} day^{-1} bar^{-1}	
sample	RH/%	thickness/ μm	OTR/cm^3 m^{-2} day^{-1} bar^{-1}	PET foil + coating	coating
neat PET	50	100	15	1.5×10^{2}	
neat polyurethane	50	80	11.6	2.1×10^{2}	4.1×10^{2}
nanocomposite	50	1.5	1.0×10^{-2}	1.0×10^{-1}	1.4×10^{-3}
	0	1.5	3.7×10^{-3}	3.8×10^{-2}	5.6×10^{-4}

[a] The coating permeability was decoupled from the total values using a method described in the literature.[26]

prototype at Mocon Inc., USA. Relative permeabilities normalized to 10 μm thick films in comparison with neat polyurethane are given in Figure 3b).

It is obvious that the nanocomposite coating led to a significant decrease of the oxygen transmission. Furthermore, the nanocomposite coating is quite insusceptible to humidity. The OTR values for 0% and 50% RH differ by a factor of 2. To underline the good water vapor barrier, WVTR measurements were conducted on neat PET as well as on the nanocomposite samples on our in-house equipment. At 50% RH PET exhibited a WVTR of 3.7 g m^{-2} day^{-1}, whereas the nanocomposite coating was below the detection limit (<0.05 g m^{-2} day^{-1}).

The thickness of the coatings was 1.5 $\pm$ 0.3 μm in the case of the nanocomposite (Figure 3a) and 80 $\pm$ 5 μm in the case of neat polyurethane. Table 1 lists the measured OTR values together with the permeability for PET foil, for the nanocomposite coating, and for the neat polyurethane coating, respectively, normalized to 10 μm thickness for comparison.

From the ratio of permeability values of nanocomposite coating and neat polyurethane matrix, the relative permeability (P_{rel}) can be calculated (3.4 $\times$ 10^{-6}). According to Cussler's model (eq 1), this relative permeability corresponds to an effective aspect ratio that is about 1 order of magnitude lower than the aspect ratios derived from FBRM measurements. We assume that the remaining discrepancy might be mainly related to inclusions of dust particles (Figure S2, Supporting Information) since the film production was not conducted under clean-room conditions. Additionally, observed partial phase segregation (Figure S3, Supporting Information) of filler and polymer matrix upon film drying lead to partial restacking of the nanoplatelets, resulting in a lower effective aspect ratio. Furthermore, alterations of the polymer's free volume that are neglected in the tortuous path theory could have led to a higher permeability and therefore lower apparent effective aspect ratio. Finally, TMAEMA intercalated into hectorite shows a *d*-spacing of 17.7 Å,

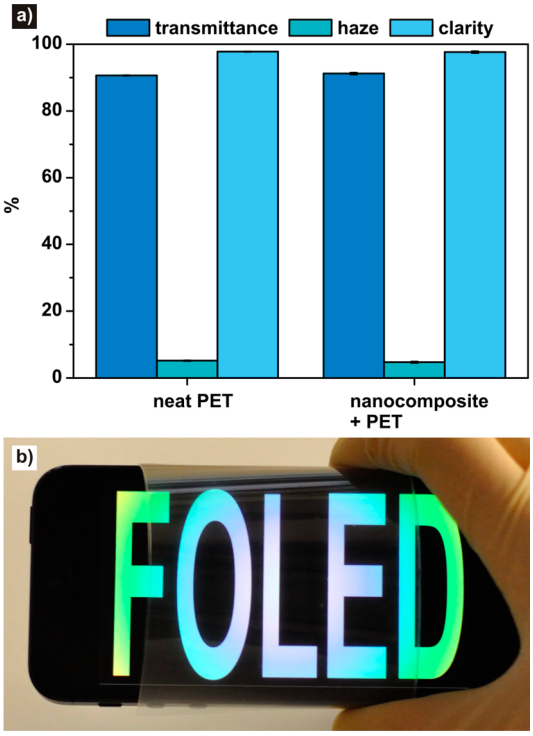

Figure 4. (a) Optical transmittance, haze, and clarity of neat PET foil and nanocomposite coating with PET foil as substrate. (b) Image of a bent nanocomposite coating on PET foil in front of a smartphone.

suggesting that the interface volume occupied by the surface modifier of the delaminated nanoplatelets is on the same order of magnitude as the volume of hectorite filler itself. The grafting density will be limited by the cation exchange capacity, and it may well be that the permeability of this interface region is larger than that of a bulk matrix and consequently will also contribute to the observed cut back in effective aspect ratio.

Nevertheless, this coating has improved the gas barrier efficiency by about 3 orders of magnitude compared to our previous best results (0.85 cm^3 10 μm m^{-2} day^{-1} bar^{-1}).[27] Moreover, while in previous work we used a special cationic polyurethane modifier that was cured by UV light and that limited the maximum filler content to some 10 vol % due to its bulky nature, here we resort to a readily available and affordable commercial two-component polyurethane system (Desmodur N 3600 and Desmophen 670 BA were provided by Bayer MaterialScience AG) and a slim monomolecular modifier that allowed filler contents of 30 vol %.

Another important feature of the synthetic hectorite-based coatings with respect to applications in display packaging is their superb optical transparency. Since some scattering is caused by surface roughness, first a clear-coat of unfilled polyurethane was applied previous to measurements. Figure 4a compares optical transmittance, clarity, and haze of neat PET foil

(substrate) and the nanocomposite coating on PET foil. The barrier films exhibited almost the same level of optical transmittance and clarity as the untreated PET foil serving as substrate. Haze values were even improved.

Additionally, to check for color fastness on displays, absorption spectra covering the range of visible light were recorded (Figure S3, Supporting Information). Comparing the spectra of PET support and the nanocomposite barrier film shows that light transmission in the visible range is limited only by the PET support.

CONCLUSION

A highly transparent, strong, and at the same time flexible nanocomposite coating on the basis of an ultrahigh aspect ratio clay was obtained applying a commercially available polyurethane matrix. Fabrication by doctor-blading is a technically benign and scalable process. At the same time, oxygen and water vapor transmission rates were among the lowest reported in the literature so far. Moreover, the coating is almost insusceptible to humidity. Altogether, this barrier coating possesses great potential for flexible display packing, *e.g.*, rollable electronic newspapers, pen-sized smartphones, and the like.

Moreover, as suggested by the recently measured in-plane moduli (~200 GPa),[28] the incorporation of these nanosheets into a tough polyurethane matrix is expected to significantly increase the Young's modulus. Preliminary nanoindentation measurements on samples of neat polyurethane and nanocomposite coated on glass slides revealed an increase of the Young's modulus from 1.0 ± 0.3 GPa (neat polyurethane) to 40 ± 5 GPa (nanocomposite). A detailed characterization of the mechanical properties of the nanocomposite films is in progress.

METHODS

Synthesis of $Na_{0.5}$-fluorohectorite. The employed $Na_{0.5}$-fluorohectorite (Na-hec) with stoichiometry $[Na_{0.5}][Li_{0.5}Mg_{2.5}][Si_4]O_{10}F_2$ was synthesized *via* melt synthesis according to an established literature procedure.[14,29,30] The material featured a cation exchange capacity (CEC) of 1.27 mval g^{-1}.

Preparation of Modifier. Trimethylammonium ethylmethacrylate iodide was used for surface modification of the hectorite. Hereby, dimethylaminoethyl methacrylate (DMAEMA, Sigma Aldrich) was quaternized according to a procedure described in the literature.[31] In a typical procedure, DMAEMA was dissolved in acetone and methyl iodide was added at a molar ratio of 1.5 compared to amino groups. Ensuring complete conversion, the mixture was stirred overnight. The precipitate was washed several times with acetone and finally dried using high vacuum. ^{1}H NMR spectroscopy revealed a quantitative quaternization.

Nanocomposite Preparation. For the surface modification of the clay a double excess of TMAEMA compared to the CEC of the Na-hec was dissolved in Millipore water, added dropwise to an aqueous suspension of Na-hec (2.5 g L^{-1}), and placed into an overhead shaker for 24 h. Afterward the clay was washed with Millipore water and the procedure was repeated. The aqueous dispersion of modified clay (O-hec) was flocculated in a 10/1 THF/butanone mixture, filtered over a 90 μm sieve, and redispersed in acetonitrile. THF, butanone, and acetonitrile were purchased from Sigma Aldrich in p.a. quality.

As a polymer matrix a two-component polyurethane system was used. The precursor polymers Desmodur N 3600 and Desmophen 670 BA were provided by Bayer MaterialScience AG, Leverkusen, Germany, and were mixed 1/1 according to the equivalent weight (ratio of reactive groups).

For preparation of the nanocomposite mixture with 50 wt % hectorite the polymer matrix and the modifier were counted as organic compound. So the 50 wt % content refers only to the neat hectorite. Matrix and modified filler were homogenized by using the SilentCrusher M (Heidolph Instruments GmbH & Co. KG) at 12 000 rpm for 2 min. Solid content (neat hectorite) was about 40 mg mL^{-1}.

The nanocomposites were deposited on PET foils *via* doctor-blading (blade speed 0.9 cm s^{-1}). The obtained films were dried at 80 °C for 3 days.

Nanocomposite Characterization. Oxygen transmission rates were acquired by Mocon (Minneapolis, MN, USA) on a Mocon OX-TRAN 2/21 XL instrument with a lower detection limit of 0.0005 cm^3 m^{-2} day^{-1} bar^{-1}. The measurements were conducted at 25 °C and relative humidities of 0% RH and 50% RH, respectively, applying the standards ASTM D-3985, ASTM F-1927, DIN 53380, JIS K-7126, and ISO CD 15105-2.

Water vapor transmission rates were measured at an Mocon PERMATRAN-W model 333 at 25 °C and a relative humidity of 50% RH. The lower detection limit of the device was 0.05 g m^{-2} day^{-1}.

SEM images were obtained on a LEO 1530 FESEM (Zeiss). The cross section polished sample was prepared by Leica Microsystems GmbH, Germany, using ion-etching.

TEM images were obtained on a JEM-2100 TEM (JEOL GmbH, Germany). Cross sections of the nanocomposite coatings were prepared with an Ion Slicer EM-09100IS (JEOL GmbH, Germany). These preparation and analytical steps were conducted by JEOL GmbH, Germany.

Transmittance, clarity, and haze of the coatings were measured on a BYK-Gardner Haze-Gard Plus, BYK Additives & Instruments (Altana AG, Germany).

Visible light transmission spectra were recorded on a Cary 300 Scan UV/vis spectrometer (Varian/Agilent Tech., CA, USA).

Nanoindentation measurements were conducted using an MFP-3DT (Asylum Research, CA, USA) equipped with a nanoindenter (Berkovich tip geometry). Hereby samples of neat polyurethane and nanocomposite film were coated onto microscopy glass slides and hardened as described above.

Conflict of Interest: The authors declare no competing financial interest.

Supporting Information Available: Supplementary Figures S1−S4. This material is available free of charge *via* the Internet at http://pubs.acs.org.

Acknowledgment. This work was supported by the German Science Foundation (SFB 840). D.A.K. thanks the elite study program "Macromolecular Science" as well as the International Graduate School "Structure, Reactivity and Properties of Oxide Materials" within the Elite Network of Bavaria (ENB) for ongoing support. Bayer MaterialScience AG is gratefully acknowledged for providing polymer samples. We are particularly indebted to Dr. F. Richter, Bayer MaterialScience AG, Leverkusen, Germany, for valuable discussions regarding the choice of commercial polyurethane system. The authors would also like to thank Paul Lippke Handels-GmbH, Germany, and Mocon Inc., USA, for conducting the permeation measurements at the SuperOxTran device. The authors thank JEOL GmbH, Germany, for the preparation and analytics of the TEM samples.

REFERENCES AND NOTES

1. Lange, J.; Wyser, Y. Recent Innovations in Barrier Technologies for Plastic Packaging - a Review. *Packag. Technol. Sci.* **2003**, *16*, 149–158.
2. Arora, A.; Padua, G. W. Review: Nanocomposites in Food Packaging. *J. Food Sci.* **2010**, *75*, 43–49.
3. Choi, M. C.; Kim, Y.; Ha, C. S. Polymers for Flexible Displays: From Material Selection to Device Applications. *Prog. Polym. Sci.* **2008**, *33*, 581–630.
4. Lewis, J. Material Challenge for Flexible Organic Devices. *Mater. Today* **2006**, *9*, 38–45.
5. Logothetidis, S. Flexible Organic Electronic Devices: Materials, Process and Applications. *Mater. Sci. Eng. B* **2008**, *152*, 96–104.
6. Burrows, P. E.; Graff, G. L.; Gross, M. E.; Martin, P. M.; Shi, M. K.; Hall, M.; Mast, E.; Bonham, C.; Bennett, W.; Sullivan, M. B. Ultra Barrier Flexible Substrates for Flat Panel Displays. *Displays* **2001**, *22*, 65–69.
7. Kumar, R. S.; Auch, M.; Ou, E.; Ewald, G.; Jin, C. S. Low Moisture Permeation Measurement through Polymer Substrates for Organic Light Emitting Devices. *Thin Solid Films* **2002**, *417*, 120–126.
8. Tang, Z. Y.; Kotov, N. A.; Magonov, S.; Ozturk, B. Nanostructured Artificial Nacre. *Nat. Mater.* **2003**, *2*, 413–418.
9. Podsiadlo, P.; Kaushik, A. K.; Arruda, E. M.; Waas, A. M.; Shim, B. S.; Xu, J. D.; Nandivada, H.; Pumplin, B. G.; Lahann, J.; Ramamoorthy, A.; *et al*. Ultrastrong and Stiff Layered Polymer Nanocomposites. *Science* **2007**, *318*, 80–83.
10. DeRocher, J. P.; Gettelfinger, B. T.; Wang, J. S.; Nuxoll, E. E.; Cussler, E. L. Barrier Membranes With Different Sizes of Aligned Flakes. *J. Membr. Sci.* **2005**, *254*, 21–30.
11. Möller, M. W.; Handge, U. A.; Kunz, D. A.; Lunkenbein, T.; Altstädt, V.; Breu, J. Tailoring Shear-Stiff, Mica-Like Nanoplatelets. *ACS Nano* **2010**, *4*, 717–724.
12. Kalo, H.; Möller, M. W.; Ziadeh, M.; Dolejš, D.; Breu, J. Large Scale Melt-Synthesis in an Open Crucible of Na-Fluorohectorite with Superb Charge Homogeneity and Particle Size. *Appl. Clay Sci.* **2010**, *48*, 39–45.
13. Kalo, H.; Möller, M. W.; Kunz, D. A.; Breu, J. How to Maximize the Aspect Ratio of Clay Nanoplatelets. *Nanoscale* **2012**, *4*, 5633–5639.
14. Stöter, M.; Kunz, D. A.; Schmidt, M.; Hirsemann, D.; Kalo, H.; Putz, B.; Senker, J.; Breu, J. Nanoplatelets of Sodium Hectorite Showing Aspect Ratios of 20000 and Superior Purity. *Langmuir* **2013**, *29*, 1280–1285.
15. Suter, J. L.; Coveney, P. V.; Greenwell, H. C.; Thyveetil, M. A. Large-Scale Molecular Dynamics Study of Montmorillonite Clay: Emergence of Undulatory Fluctuations and Determination of Material Properties. *J. Phys. Chem. C* **2007**, *111*, 8248–8259.
16. Kalo, H.; Milius, W.; Breu, J. Single Crystal Structure Refinement of One- and Two-Layer Hydrate of Sodium-Fluorohectorite. *RSC Adv.* **2012**, *2*, 8452–8459.
17. Choudalakis, G.; Gotsis, A. D. Free Volume and Mass Transport in Polymer Nanocomposites. *Curr. Opin. Colloid Interface Sci.* **2012**, *17*, 132–140.
18. Kotov, N. A.; Haraszti, T.; Turi, L.; Zavala, G.; Geer, R. E.; Dekany, I.; Fendler, J. H. Mechanism of and Defect Formation in the Self-Assembly of Polymeric Polycation-Montmorillonite Ultrathin Films. *J. Am. Chem. Soc.* **1997**, *119*, 6821–6832.
19. Podsiadlo, P.; Michel, M.; Lee, J.; Verploegen, E.; Kam, N. W. S.; Ball, V.; Lee, J.; Qi, Y.; Hart, A. J.; Hammond, P. T.; *et al*. Exponential Growth of LBL Films with Incorporated Inorganic Sheets. *Nano Lett.* **2008**, *8*, 1762–1770.
20. Priolo, M. A.; Gamboa, D.; Holder, K. M.; Grunlan, J. C. Super Gas Barrier of Transparent Polymer-Clay Multi layer Ultrathin Films. *Nano Lett.* **2010**, *10*, 4970–4974.
21. Priolo, M. A.; Holder, K. M.; Greenlee, S. M.; Grunlan, J. C. Transparency, Gas Barrier, and Moisture Resistance of Large-Aspect-Ratio Vermiculite Nanobrick Wall Thin Films. *ACS Appl. Mater. Interfaces* **2012**, *4*, 5529–5533.
22. Yang, Y. H.; Bolling, L.; Priolo, M. A.; Grunlan, J. C. Super Gas Barrier and Selectivity of Graphene Oxide-Polymer Multilayer Thin Films. *Adv. Mater.* **2013**, *25*, 503–508.
23. Heath, A. R.; Fawell, P. D.; Bahri, P. A.; Swift, J. D. Estimating Average Particle Size by Focused Beam Reflectance Measurement (FBRM). *Part. Part. Syst. Charact.* **2002**, *19*, 84–95.
24. Goossens, D. Techniques to Measure Grain-Size Distributions of Loamy Sediments: A Comparative Study of Ten Instruments for Wet Analysis. *Sedimentology* **2008**, *55*, 65–96.
25. Möller, M. W.; Lunkenbein, T.; Kalo, H.; Schieder, M.; Kunz, D. A.; Breu, J. Barrier Properties of Synthetic Clay with a Kilo-Aspect Ratio. *Adv. Mater.* **2010**, *22*, 5245–5249.
26. Roberts, A. P.; Henry, B. M.; Sutton, A. P.; Grovenor, C. R. M.; Briggs, G. A. D.; Miyamoto, T.; Kano, A.; Tsukahara, Y.; Yanaka, M. Gas Permeation in Silicon-Oxide/Polymer (SiOx/PET) Barrier Films: Role of the Oxide Lattice, Nano-Defects and Macro-Defects. *J. Membr. Sci.* **2002**, *208*, 75–88.
27. Möller, M. W.; Kunz, D. A.; Lunkenbein, T.; Sommer, S.; Nennemann, A.; Breu, J. UV-Cured, Flexible, and Transparent Nanocomposite Coating with Remarkable Oxygen Barrier. *Adv. Mater.* **2012**, *24*, 2142–2147.
28. Kunz, D. A.; Erath, J. Kluge, D.; Thurn, H.; Putz, B.; Fery, A.; Breu, J. In-Plane Modulus of Singular 2:1-Clay Lamellae Applying a Simple Wrinkling Technique. Unpublished work.
29. Breu, J.; Seidl, W.; Stoll, A. J.; Lange, K. G.; Probst, T. U. Charge Homogeneity in Synthetic Fluorohectorite. *Chem. Mater.* **2001**, *13*, 4213–4220.
30. Malikova, N.; Cadene, A.; Dubois, E.; Marry, V.; Durand-Vidal, S.; Turq, P.; Breu, J.; Longeville, S.; Zanotti, J. M. Water Diffusion in a Synthetic Hectorite Clay Studied by Quasi-Elastic Neutron Scattering. *J. Phys. Chem. C* **2007**, *111*, 17603–17611.
31. Plamper, F. A.; Schmalz, A.; Penott-Chang, E.; Drechsler, M.; Jusufi, A.; Ballauff, M.; Muller, A. H. E. Synthesis and Characterization of Star-Shaped Poly(*N*,*N*-dimethylaminoethyl methacrylate) and its Quaternized Ammonium Salts. *Macromolecules* **2007**, *40*, 5689–5697.